IVYSPRING INTERNATIONAL PUBLISHER

JOURNAL OF CANCER

2026; 17(12): 2126-2136. doi: 10.7150/jca.142715

Research Paper

Co-targeting Aurora Kinase A and DNA Damage Response Pathways Enhances Apoptotic Cell Death in Cholangiocarcinoma Cells

Benchamart Moolmuang[1], Mathuros Ruchirawat[1,2]✉

1. Laboratory of Chemical Carcinogenesis, Chulabhorn Research Institute, Bangkok 10210, Thailand.
2. Center of Excellence on Environmental Health and Toxicology, Office of the Permanent Secretary, Ministry of Higher Education, Science, Research and Innovation, Bangkok 10400, Thailand.

✉ Corresponding author: Mathuros Ruchirawat, Tel: +662-553-8555 ext. 8537; Fax: +6625538527; E-mail address: mathuros@cri.or.th.

© 2026 The Author(s). This is an open access article distributed under the Creative Commons Attribution 4.0 International Licence, subject to the Publisher's Terms of Use at https://ivyspring.com/terms.

Received: 2026.08.18; Accepted: 2026.10.10; Published: 2026.11.13

Abstract

Cholangiocarcinoma (CCA) is a highly aggressive malignancy with limited therapeutic options and poor clinical outcomes. Aurora kinase A (AURKA), a key regulator of mitotic progression, is frequently dysregulated in human cancers and represents a promising therapeutic target. This study investigated the growth-inhibitory effects of AURKA inhibition and evaluated whether co-targeting the DNA damage response (DDR) pathway could enhance these effects in CCA cells. Four human CCA cell lines were treated with the pan-Aurora kinase inhibitor VX-680 or the selective AURKA inhibitor alisertib. Cell viability, cell cycle progression, apoptosis, and the expression of DNA damage- and apoptosis-related proteins were assessed. Both VX-680 and alisertib inhibited CCA cell proliferation in a dose- and time-dependent manner. Alisertib induced G2/M phase arrest and apoptosis in all CCA cell lines. Combined treatment with alisertib or the polo-like kinase 1 (PLK1) inhibitor BI2536 and the ATM inhibitor KU55933 or the ATR inhibitor VE-821 further enhanced apoptotic cell death, particularly in the most responsive KKU055 cells. Mechanistically, dual inhibition markedly increased γH2AX accumulation and PARP cleavage in a cell line-dependent manner, with the most pronounced effects observed in KKU055 cells, indicating enhanced DNA damage and apoptotic cell death. These findings demonstrate a functional interplay between mitotic kinase signaling and DDR pathways in CCA cells and suggest that their concurrent inhibition enhances growth-inhibitory and pro-apoptotic responses.

Keywords: cholangiocarcinoma, Aurora kinase A, polo-like kinase 1, DNA damage response, apoptosis

Introduction

Cholangiocarcinoma (CCA) is a highly heterogeneous and aggressive malignancy arising from the epithelial lining of the bile ducts. It represents a major health burden in Southeast Asia, particularly in Thailand, where its incidence remains among the highest worldwide. Based on anatomical location, CCA is classified into three subtypes: intrahepatic (iCCA), perihilar (pCCA), and distal (dCCA), each exhibiting distinct characteristics, prognoses, and treatment approaches. Although diagnostic and treatment approaches have improved, patients with advanced CCA continue to face poor outcomes because of late-stage diagnosis, high metastatic potential, and limited responsiveness to conventional chemotherapy [1, 2]. Complete surgical resection is the standard curative treatment for CCA; however, most patients present with advanced or unresectable disease. In these cases, systemic chemotherapy, molecularly targeted therapies, and immunotherapy have emerged as important therapeutic strategies; however, clinical outcomes remain unsatisfactory because of limited response rates, acquired resistance, and disease progression [3, 4]. Recent evidence suggests that chronic inflammatory signaling and oxidative stress contribute to cholangiocarcinogenesis by inducing genomic instability through the accumulation of DNA damage and impairment of DNA repair mechanisms. Furthermore, alterations in

DNA damage response (DDR) pathways have emerged as important drivers of CCA development and potential therapeutic vulnerabilities. Despite substantial genomic stress, CCA cells frequently evade apoptosis through the activation of multiple pro-survival signaling networks, thereby promoting tumor progression and treatment resistance [5]. These findings underscore the urgent need to identify novel molecular targets and develop more effective therapeutic strategies, particularly those that exploit vulnerabilities in mitotic regulation and DDR pathways, to improve outcomes for patients with CCA.

Aurora kinases are a family of serine/threonine kinases that coordinate multiple events during mitosis, including centrosome maturation, spindle assembly, chromosome alignment, and cytokinesis. The Aurora kinase family comprises three members: aurora kinase A (AURKA), aurora kinase B (AURKB), and aurora kinase C (AURKC), which share a highly conserved catalytic kinase domain but exhibit distinct tissue distribution patterns and biological functions during cell division [6, 7]. Among the three Aurora kinases, AURKA has attracted the greatest research interest because of its frequent dysregulation in cancer and its involvement in multiple oncogenic signaling pathways. AURKA is frequently amplified and overexpressed in a broad spectrum of human malignancies, including breast, colorectal, ovarian, gastric, pancreatic, and hepatobiliary cancers, where its dysregulation promotes chromosomal instability, tumor progression, and poor clinical outcomes [6, 8, 9]. In CCA, evidence regarding the role of AURKA remains limited. Ding *et al*. demonstrated that several mitotic checkpoint genes, including AURKA, are aberrantly upregulated in CCA and that pharmacological inhibition of AURKA using alisertib or siRNA-mediated knockdown suppresses cell proliferation, induces G2/M phase arrest, and promotes apoptosis in CCA cells [10]. In parallel, our previous study identified polo-like kinase 1 (PLK1) as a critical regulator of CCA cell survival and proliferation, showing that PLK1 inhibition markedly impaired CCA cell growth and promoted apoptotic cell death [11]. Given that AURKA and PLK1 function cooperatively during mitotic progression and are closely involved in maintaining genomic stability, these observations suggest that CCA cells may be particularly dependent on mitotic kinase signaling for survival. Therefore, this study aimed to investigate the functional interplay between mitotic kinases and DDR signaling in CCA cells and to determine whether simultaneous inhibition of AURKA or PLK1 and DDR pathways could enhance DNA damage accumulation and promote apoptotic cell death. Understanding this interaction may provide a rationale for the development of novel combination therapeutic strategies for CCA.

Materials and Methods

Cell culture and materials

CCA cell lines established from Thai patients, including KKU055, KKU100 [12], KKU213A, and HuCCA1 [13], were used in this study. KKU055, KKU100, and KKU213A cells were obtained from the Japanese Collection of Research Bioresources Cell Bank (JCRB), whereas HuCCA1 cells were generously provided by Dr. Stitaya Sirisinha, Mahidol University, Thailand. KKU055, KKU213A, and HuCCA1 were derived from patients with intrahepatic CCA, while KKU100 cells were established from a patient with extrahepatic CCA. KKU055, KKU100, and KKU213A cells were maintained in Dulbecco's modified Eagle's medium (DMEM; HyClone, Cytiva, Marlborough, MA, USA), and HuCCA1 cells were maintained in Ham's F12 medium (HyClone, Cytiva, Marlborough, MA, USA). All cell culture media were supplemented with 10% fetal bovine serum (FBS; Gibco, Thermo Fisher Scientific, Waltham, MA, USA) and 1% penicillin-streptomycin (Gibco, Thermo Fisher Scientific). Cells were cultured at 37 ˚C in a humidified incubator containing 5% CO_2. All CCA cell lines used in this study were previously authenticated by STR profiling at CLS Cell Lines Service GmbH (cat. no. 900154; August 2023). Authentication results showed complete concordance with the reference profiles of HuCCA1, KKU100, and KKU213A cells (100% match), whereas KKU055 exhibited a 93.8% match. The authenticated cell lines have been continuously maintained and used in the present study.

Alisertib (HY-10971) and BI2536 (HY-50698) were purchased from MedChemExpress (Monmouth Junction, NJ, USA). VX-680 (SML2158), VE-821 (SML1415), and KU55933 (SML1190) were purchased from Sigma-Aldrich (St. Louis, MO, USA). Stock solutions of alisertib, VX-680, BI2536, VE-821, and KU55933 were prepared in dimethyl sulfoxide (DMSO) and stored at −80°C according to the manufacturer's recommendations. The final DMSO concentration in culture medium did not exceed 0.1% (v/v). Primary antibodies against PARP (#9542), phospho-Histone H2AX (Ser139; γH2AX; #9718), and GAPDH (#8884) were purchased from Cell Signaling Technology (Danvers, MA, USA). Horseradish peroxidase (HRP)-conjugated goat anti-rabbit IgG (#7074; Cell Signaling Technology) was used as the secondary antibody.

Cell viability assay

Cell viability was determined using the MTT assay. Briefly, 1 × 10^4 cells were seeded in triplicate in 24-well plates and treated with various concentrations of VX-680 or alisertib for 24, 48, or 72 h. Following treatment, the culture medium was replaced with fresh medium containing 0.5 mg/ml MTT (prepared from a 5 mg/ml stock solution; M2128, MilliporeSigma, St. Louis, MO, USA), and the cells were incubated at 37°C for 1.5 h. The resulting formazan crystals were dissolved in DMSO, and absorbance was measured at 540 nm using a Victor Nivo microplate reader (PerkinElmer, Waltham, MA, USA). Cell viability was expressed as a percentage relative to that of vehicle-treated control cells. IC50 values were determined from cell viability data using nonlinear regression analysis in GraphPad Prism 9.0. Experiments were performed in at least three independent biological replicates.

Cell cycle analysis

Cell cycle distribution was analyzed using a Muse Cell Cycle Assay Kit (MCH100106; Luminex Corporation, Austin, TX, USA) according to the manufacturer's instructions. Briefly, 1.5 × 10^5 cells were cultured in 6-well plates. After an overnight incubation, the cells were treated with the IC50 concentration of alisertib for 24 h. Following treatment, cells were harvested by trypsinization, washed with phosphate-buffered saline (PBS), and fixed in ice-cold 70% ethanol at −20°C overnight. Following fixation, cells were washed with PBS, centrifuged at 300 × g for 5 min at room temperature, and resuspended in Muse Cell Cycle Reagent. After incubation in the dark for 30 min at room temperature, samples were analyzed using a Muse Cell Analyzer (Luminex Corporation). The percentages of cells in the G0/G1, S, and G2/M phases were determined based on DNA content. All experiments were performed independently in biological triplicate.

Detection of cell apoptosis

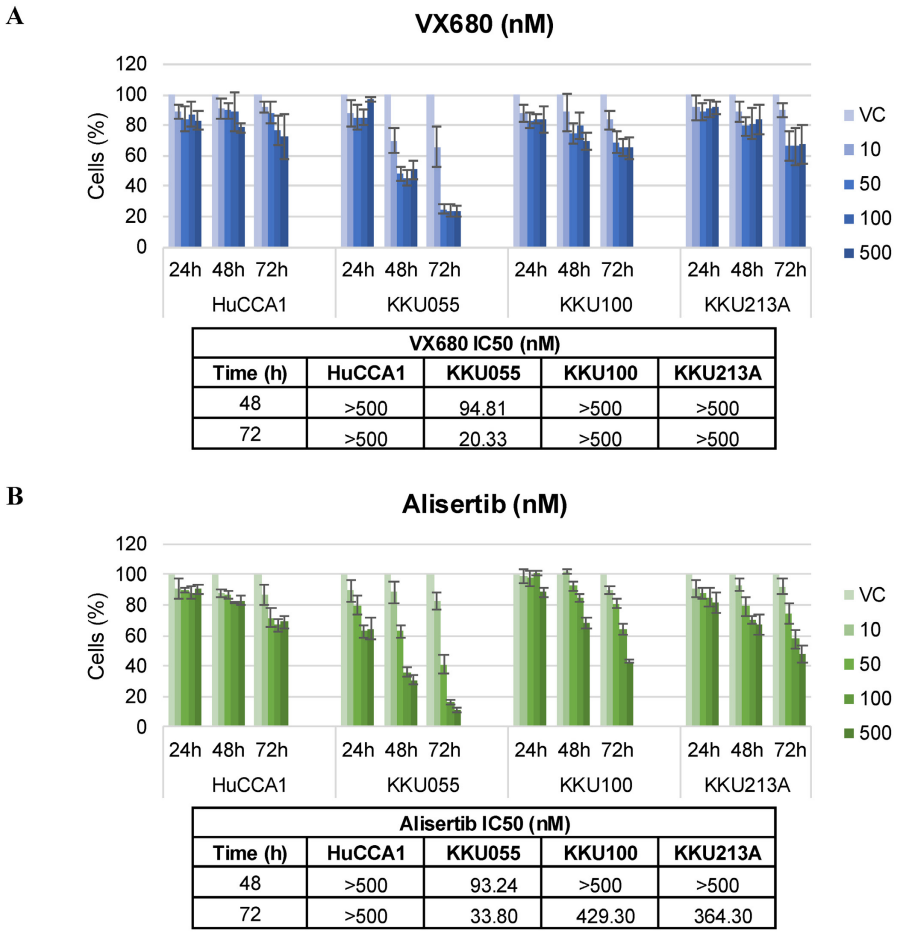
Apoptosis was quantified using a Muse Annexin V and Dead Cell Kit (MCH100105; Luminex Corporation, Austin, TX, USA) according to the manufacturer's instructions. Briefly, 1.5 × 10^5 cells were seeded in 6-well plates and allowed to adhere overnight. Cells were then treated with alisertib at its IC50 concentration, either alone or in combination with other agents, for 48 h. Following treatment, both floating and adherent cells were collected, with adherent cells harvested by trypsinization. Cells were centrifuged at 300 × g for 5 min, and the pellets were resuspended in culture medium containing 1% FBS. Equal volumes of cell suspension and Muse Annexin V & Dead Cell reagent were mixed and incubated for 20 min at room temperature in the dark. Samples were subsequently analyzed using a Muse Cell Analyzer (Luminex Corporation). The percentages of live, early apoptotic, late apoptotic, total apoptotic, and dead cells were determined using the manufacturer's analysis software. All experiments were performed independently in biological triplicate.

Western blot analysis

Treated cells were washed with ice-cold PBS and lysed in RIPA buffer (50 mM Tris-HCl, pH 7.4, 150 mM NaCl, 1% NP-40, 0.25% sodium deoxycholate, and 1 mM EDTA) supplemented with Halt Protease and Phosphatase Inhibitor Cocktail (78440; Thermo Fisher Scientific). Cell lysates were centrifuged at 14,000 × g for 15 min at 4°C, and protein concentrations were determined using the Bradford assay (B6916; MilliporeSigma) according to the manufacturer's instructions. Equal amounts of protein (20 µg) were resolved by 12% SDS-PAGE and transferred to polyvinylidene fluoride (PVDF) membranes (Immobilon; MilliporeSigma). Membranes were blocked with 5% non-fat dry milk in Tris-buffered saline containing 0.1% Tween-20 (TBST) for 1 h at room temperature and incubated overnight at 4°C with the indicated primary antibodies diluted in either 4% bovine serum albumin (BSA; Santa Cruz Biotechnology) or 5% non-fat dry milk in TBST. After washing with TBST, membranes were incubated with HRP-conjugated secondary antibodies for 2 h at room temperature. Immunoreactive bands were detected using the ECL Plus Western Blotting Detection System (Cytiva) and visualized using a G:BOX imaging system (Syngene, Cambridge, UK). Band intensities were quantified using ImageJ software (version 1.53; National Institutes of Health, Bethesda, MD, USA) and normalized to GAPDH.

Statistical analysis

Statistical analyses were performed using SPSS software (version 30.0; IBM Corp., Armonk, NY, USA). Differences between the two groups were analyzed using an unpaired two-tailed Student's t-test. Comparisons among multiple groups were performed using one-way analysis of variance (ANOVA) followed by Tukey's honestly significant difference (HSD) post hoc test. A P-value < 0.05 was considered statistically significant.



VX680 IC50 (nM)				
Time (h)	HuCCA1	KKU055	KKU100	KKU213A
48	>500	94.81	>500	>500
72	>500	20.33	>500	>500

Alisertib IC50 (nM)				
Time (h)	HuCCA1	KKU055	KKU100	KKU213A
48	>500	93.24	>500	>500
72	>500	33.80	429.30	364.30

Figure 1. Aurora kinase inhibitors suppress cholangiocarcinoma cell viability. HuCCA1, KKU100, KKU055, and KKU213A cells were treated with increasing concentrations (10 - 500 nM) of (A) VX-680, a pan-Aurora kinase inhibitor, or (B) alisertib, a selective Aurora kinase A inhibitor, for 24, 48, and 72 h. Cell viability was determined using the MTT assay. Data are presented as mean ± SD from three independent experiments. IC50 values at 48 and 72 h were calculated by nonlinear regression analysis and are shown below each graph. IC50 values exceeding the highest tested concentration (500 nM) are reported as >500 nM. Corresponding extrapolated IC50 values are provided in Supplementary Tables S1 and S2 for VX-680 and alisertib, respectively.

Results

1. Aurora kinase inhibitors VX-680 and alisertib inhibit cholangiocarcinoma cell proliferation

To determine the effects of Aurora kinase inhibition on the viability of CCA cells, two inhibitors were tested: VX-680, a pan-Aurora kinase inhibitor targeting Aurora kinases A, B, and C, and alisertib, a selective Aurora kinase A inhibitor. Four CCA cell lines (HuCCA1, KKU100, KKU055, and KKU213A) were treated with VX-680 or alisertib at concentrations ranging from 10 to 500 nM for 24, 48, and 72 h. Cell viability was subsequently measured using an MTT assay. As shown in Figure 1, both VX-680 (Figure 1A) and alisertib (Figure 1B) reduced cell viability in all four CCA cell lines in a dose- and time-dependent manner. The half-maximal inhibitory concentration (IC50) values are summarized in the table below the graphs. HuCCA1 and KKU213A cells exhibited limited sensitivity to VX-680 and alisertib, with IC50 values exceeding the highest tested concentration (500 nM) at several time points. Moreover, KKU100 cells exhibited limited sensitivity to VX-680, and the IC50 could not be determined within the tested concentration range at 72 h. Consequently, these IC50 values are reported as > 500 nM. Notably, the sensitivity to both inhibitors varied among the cell lines, with KKU055 exhibiting the lowest IC50 values and HuCCA1 the highest. Alisertib was chosen for further investigation because its higher selectivity for AURKA enables a more precise evaluation of AURKA-driven signaling in CCA.

2. Alisertib induces G2/M cell cycle arrest in cholangiocarcinoma cells

Given the established role of AURKA in mitotic progression, we next examined whether alisertib affects cell cycle progression in CCA cells. Cells were treated with alisertib at the IC50 concentration specific to each cell line. After 24 h of treatment, cell cycle distribution was analyzed by flow cytometry. Figure 2

shows that alisertib treatment induced G2/M phase arrest in all four cell lines. The proportion of cells in the G2/M phase was significantly increased compared with that in vehicle-treated control cells (Figure 2A). Representative histograms of cell cycle distribution obtained using the Muse cell analyzer are shown in Figure 2B.

3. Alisertib triggers apoptotic cell death in cholangiocarcinoma cells

To determine whether alisertib induces apoptosis in CCA cells, each cell line was treated with alisertib at its respective IC50 concentration. Because prolonged mitotic arrest frequently leads to apoptotic cell death, apoptosis was evaluated following 48 h of alisertib treatment. Apoptotic cell death was evaluated by Annexin V/7-AAD double staining followed by flow cytometric analysis, which allowed discrimination among live, early apoptotic, and late apoptotic cells. As shown in Figure 3A, the percentage of total apoptotic cells (early and late apoptosis) was significantly increased in alisertib-treated cells compared with vehicle-treated control cells. Representative flow cytometry plots obtained using the Muse cell analyzer are also shown in Figure 3B.

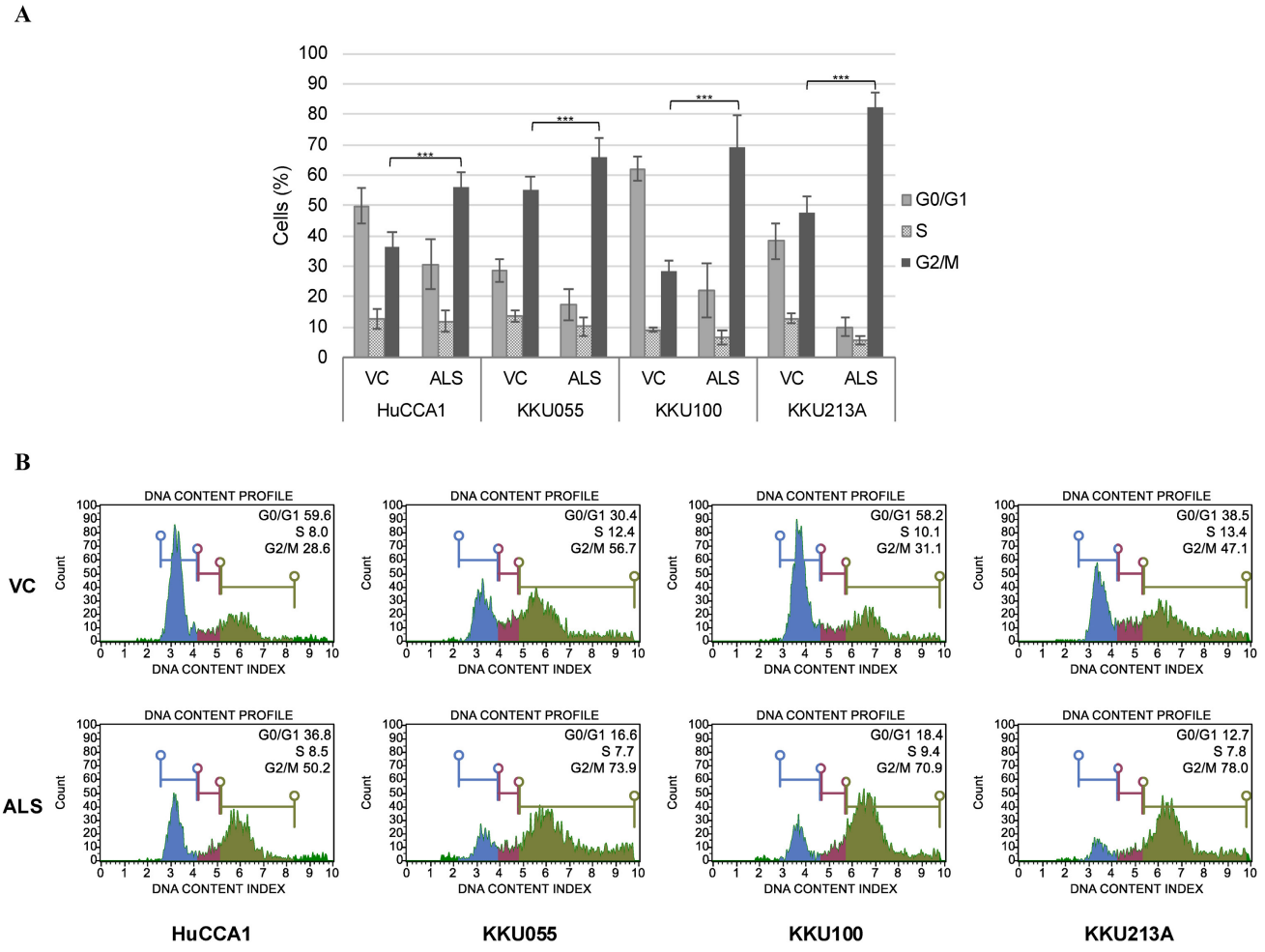


Figure 2. Alisertib induces G2/M cell cycle arrest in cholangiocarcinoma cells. CCA cells were treated with vehicle control or alisertib at IC50 concentrations specific to each cell line for 24 h. Cell cycle distribution was analyzed by flow cytometry using the Muse Cell Cycle Assay Kit. (A) Quantification of cell populations in G0/G1, S, and G2/M phases. Data are presented as the mean ± SD from three independent experiments. *** P<0.001 compared with vehicle control for the G2/M cell population. (B) Representative cell cycle histograms from a single independent experiment showing cell cycle distribution in vehicle control and alisertib-treated cells obtained using the Muse cell analyzer. VC, vehicle control; ALS, alisertib.

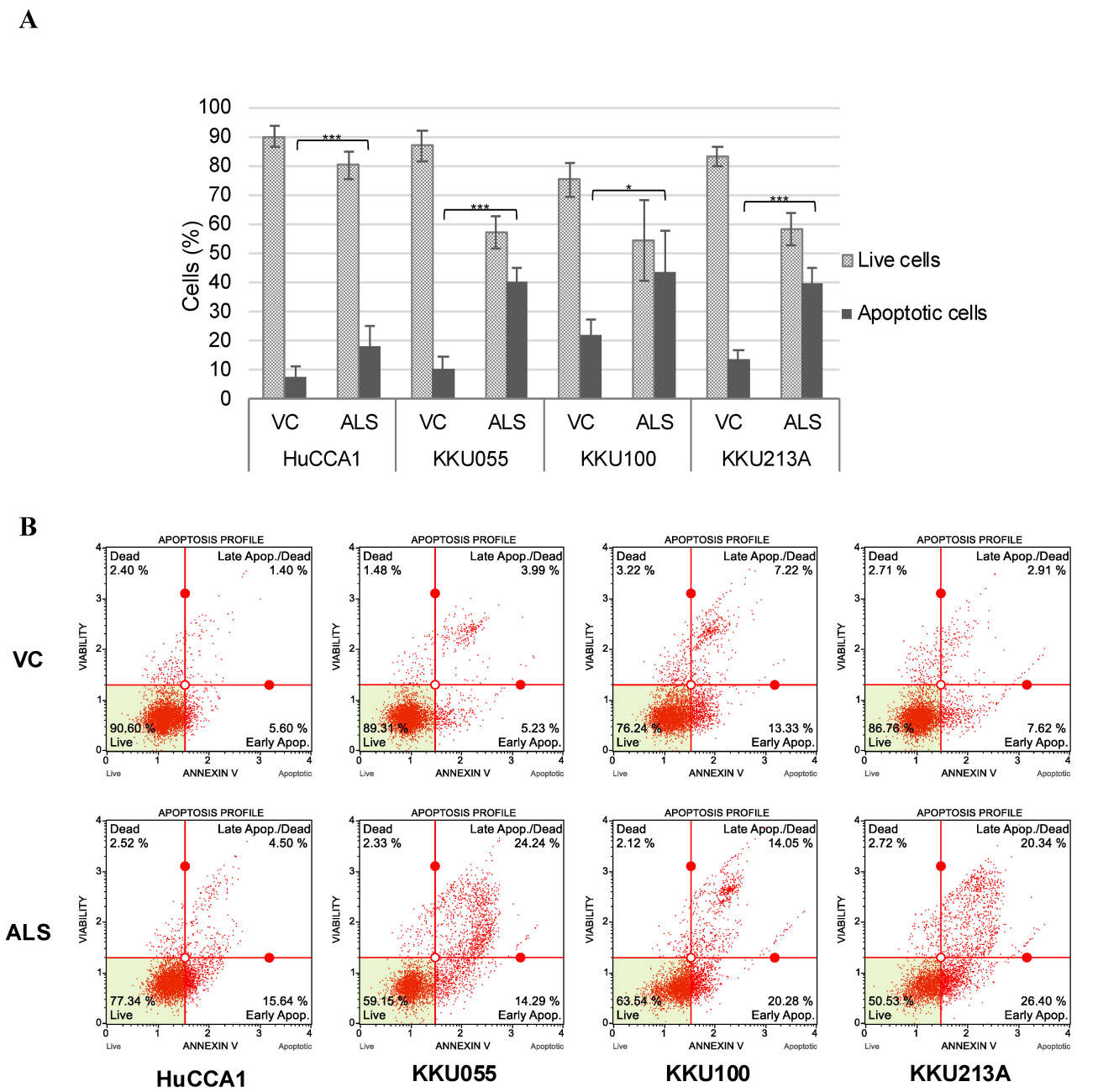


Figure 3. Alisertib induces apoptotic cell death in cholangiocarcinoma cells. CCA cells were treated with vehicle control or alisertib at the IC50 concentration specific to each cell line for 48 h. Total apoptotic cells were measured by flow cytometry using the Muse Annexin-V and Dead Cell kit. (A) Bar graphs show the percentages of live cells and total apoptotic cells (early + late apoptosis). Data are presented as mean ± SD of at least three independent experiments. *P<0.05, ***P<0.001 versus vehicle control. (B) Representative flow cytometry plots of Annexin V/7-AAD double staining from a single independent experiment showing the distribution of live, early apoptotic, late apoptotic, and dead cell populations following treatment in CCA cells. VC, vehicle control; ALS, alisertib.

4. Combined inhibition of ATM or ATR enhances apoptosis induced by AURKA or PLK1 inhibition in cholangiocarcinoma cells

Since AURKA inhibition with alisertib induced G2/M phase arrest followed by apoptotic cell death in CCA cell lines, we next investigated whether simultaneous inhibition of AURKA and DDR pathways could enhance this response. CCA cells were treated with alisertib at the IC50 concentration specific to each cell line in combination with the ATM inhibitor KU55933 or the ATR inhibitor VE-821. To determine whether this effect extended to another mitotic kinase, we also included the PLK1 inhibitor BI2536, which, as shown in our previous study, induces G2/M phase arrest and apoptosis in CCA cells. Cells were treated with vehicle, alisertib, or BI2536, alone or in combination with VE-821 (5 μM) or KU55933 (10 μM), and apoptosis was assessed after 48 h. As shown in Figure 4, the apoptotic response to

combination treatment varied among the CCA cell lines. In KKU055 cells, which were the most sensitive to AURKA and PLK1 inhibition, co-treatment with either VE-821 or KU55933 significantly increased total apoptosis compared with the corresponding single-agent treatment (Figure 4A). In KKU100 cells, co-treatment with either VE-821 or KU55933 significantly enhanced alisertib-induced apoptosis compared with alisertib alone, whereas neither combination further increased BI2536-induced apoptosis (Figure 4B). In KKU213A cells, KU55933 markedly enhanced alisertib-induced apoptosis and produced the highest apoptotic fraction among all treatment groups, while VE-821 combined with alisertib resulted in only a modest enhancement of apoptosis. On the other hand, VE-821 did not enhance BI2536-induced apoptosis, and the apoptotic fraction observed following VE-821 plus BI2536 treatment was lower than that observed with BI2536 alone (Figure 4C). In contrast, only modest increases in apoptosis were observed in HuCCA1 cells, which showed the lowest sensitivity to AURKA and PLK1 inhibition (Figure 4D).

5. Co-inhibition of ATM or ATR with AURKA or PLK1 increases γH2AX and PARP cleavage

To investigate whether enhanced apoptosis was associated with increased DNA damage, γH2AX and PARP cleavage were examined in KKU055 and HuCCA1 cells, representing the most sensitive and least sensitive cell lines, respectively. In KKU055 cells, combination treatment increased γH2AX accumulation and PARP cleavage compared with the corresponding single-agent treatment (Figure 5A), indicating increased DNA damage and apoptosis. Notably, BI2536 alone induced more pronounced γH2AX accumulation and PARP cleavage than alisertib, and these effects were further enhanced by co-treatment with ATM or ATR inhibitors. Consistent with the apoptosis data, the combination of mitotic kinase and DDR inhibition produced the strongest molecular response in KKU055 cells. In contrast, HuCCA1 cells exhibited a distinct and less pronounced response (Figure 5B). KU55933 treatment increased γH2AX levels both as a single agent and in combination with alisertib or BI2536. However, enhanced γH2AX accumulation was not consistently accompanied by increased PARP cleavage. Moreover, the effects of combination treatment on γH2AX and cleaved PARP expression varied depending on the inhibitor combination, with several combinations producing comparable or lower levels of γH2AX and cleaved PARP than the corresponding single-agent treatments. These findings suggest that the molecular response to combined mitotic kinase and DDR inhibition is cell line-dependent and is more pronounced in the drug-sensitive KKU055 cells than in the relatively resistant HuCCA1 cells.

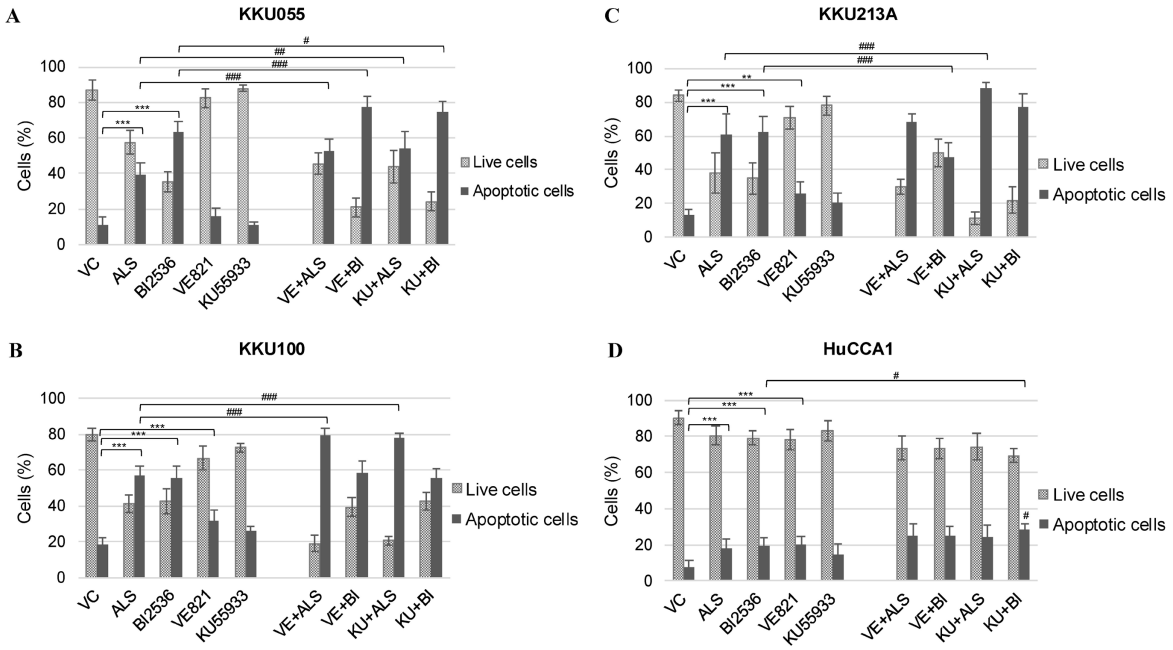


Figure 4. Co-inhibition of ATM or ATR with AURKA or PLK1 enhances apoptotic cell death in cholangiocarcinoma cells. (A) KKU055, (B) KKU100, (C) KKU213A, and (D) HuCCA1 cells were treated for 48 h with vehicle control, AURKA inhibitor alisertib, PLK1 inhibitor BI2536, ATR inhibitor VE-821, ATM inhibitor KU55933, VE-821+alisertib, VE-821+BI2536, KU55933+alisertib, or KU55933+BI2536. The IC50 concentrations of alisertib or BI2536 specific to each cell line were used, whereas VE-821 (5 μM) and KU55933 (10 μM) were administered at fixed concentrations. Total apoptotic cells were assessed by flow cytometry using the Muse Annexin-V and Dead Cell kit. Bar graphs show the percentages of total apoptotic (early + late) and live cells. Data are presented as mean ± SD of at least three independent experiments. *P < 0.05, **P < 0.01, ***P < 0.001 versus control. #P < 0.05, ##P < 0.01 versus corresponding single-agent treatment as indicated by brackets. VC, vehicle control; ALS, alisertib; BI, BI2536; VE, VE-821; KU, KU55933.

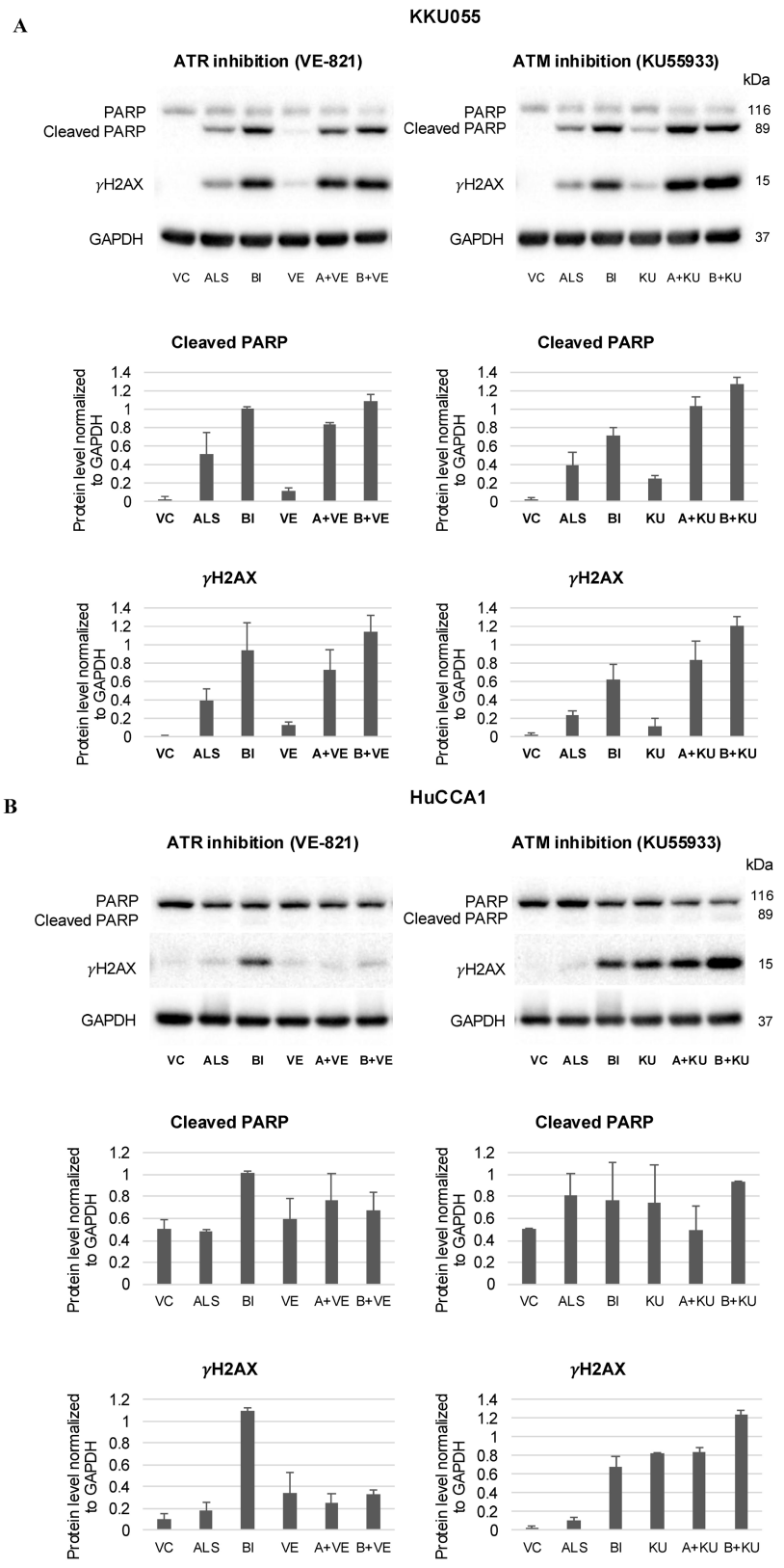


Figure 5. Combined inhibition of ATM or ATR with AURKA or PLK1 increases γH2AX accumulation and PARP cleavage in CCA cells. (A) KKU055 and (B) HuCCA1 cells were treated for 24 h with vehicle control, alisertib, BI2536, VE-821, alisertib+VE-821, or BI2536+VE-821 (ATR inhibition set), and with vehicle control, alisertib, BI2536, KU55933, alisertib+KU55933, or BI2536+KU55933 (ATM inhibition set). The IC50 concentrations of alisertib or BI2536 specific to each cell line were used, whereas VE-821 (5 μM) and KU55933 (10 μM) were administered at fixed concentrations. Whole-cell lysates were subjected to western blot analysis to detect the expression of γH2AX, full-length PARP, and cleaved PARP, with GAPDH serving as a loading control. Bar graphs represent the densitometric quantification of protein expression levels. Cleaved PARP and γH2AX levels were normalized to GAPDH. Data are presented as mean ± SD from at least three independent experiments. Original uncropped membrane section images and corresponding molecular weight markers for these Western blot analyses shown in this figure are provided in Supplementary Figures S1 and S2. The molecular weights of the detected proteins are indicated in kDa. VC, vehicle control; ALS, alisertib; BI, BI2536; VE, VE-821; KU, KU55933.

Discussion

Cholangiocarcinoma is a highly aggressive malignancy associated with limited therapeutic options and poor clinical outcomes. An incomplete understanding of the molecular mechanisms underlying CCA progression has hindered the development of effective targeted therapies, highlighting the need to identify novel therapeutic vulnerabilities. Mitotic kinases have emerged as promising therapeutic targets because they regulate cell cycle progression, chromosome segregation, and genomic stability, processes that are frequently dysregulated in cancer.

Aurora kinase A is a key regulator of mitotic progression and contributes to multiple hallmarks of cancer through its roles in centrosome maturation, spindle assembly, chromosome segregation, and cell cycle regulation. Aberrant AURKA expression has been implicated in tumor initiation and progression in various malignancies. In the present study, we investigated the effects of Aurora kinase inhibition in four CCA cell lines (KKU055, KKU100, KKU213A, and HuCCA1) using both a pan-Aurora kinase inhibitor (VX-680) and a selective AURKA inhibitor (alisertib). VX-680 and alisertib have previously demonstrated antitumor activity in multiple cancer types [14-18]. Consistent with these reports, both VX-680 and alisertib inhibited CCA cell proliferation, although the magnitude of response varied among the cell lines examined (Figure 1). Furthermore, alisertib induced G2/M phase cell cycle arrest (Figure 2) and promoted apoptotic cell death (Figure 3), supporting the critical role of AURKA in maintaining CCA cell survival. The observed antiproliferative effect of AURKA inhibition is consistent with our previous findings demonstrating that inhibition of another mitotic kinase, polo-like kinase 1 (PLK1), suppresses CCA cell growth [11]. Because mitotic kinases and DDR pathways are both essential for maintaining genome integrity, we next investigated whether simultaneous targeting of these pathways could enhance the apoptotic response induced by mitotic kinase inhibition. Previous studies have shown that inhibition of ATM or ATR sensitizes CCA cells to DNA-damaging agents and enhances cytotoxicity [19]. However, the potential functional interaction between AURKA signaling and DDR pathways has not been explored in CCA. Emerging evidence from other cancer models suggests that AURKA contributes to genomic stability and participates in the regulation of DNA repair processes [9]. Given the critical role of ATR signaling in protecting cancer cells from replication stress, we investigated whether inhibition of ATM or ATR signaling could enhance the cytotoxic effects of AURKA or PLK1 inhibition. The concentrations of KU55933 and VE-821 were selected based on our previous study, in which these doses produced approximately 50% growth inhibition in the most sensitive CCA cell line [20]. The rationale for this combination strategy was based on the differential sensitivity of CCA cell lines to alisertib treatment, suggesting that some cells may possess compensatory survival mechanisms that limit the cytotoxic effects of AURKA inhibition.

Our results demonstrated that co-inhibition of ATM or ATR significantly enhanced cell death induced by AURKA or PLK1 inhibition in CCA cells (Figure 4). Notably, KKU055 cells exhibited the most pronounced response, whereas the effects were more variable in the other cell lines. In KKU055 cells, inhibition of either ATM or ATR consistently enhanced the pro-apoptotic effects of AURKA or PLK1 inhibitors. In KKU100 cells, both ATR and ATM inhibition significantly increased alisertib-induced apoptosis, whereas neither inhibitor further enhanced apoptosis induced by BI2536. Similarly, in KKU213A cells, the strongest apoptotic response was observed following co-treatment with KU55933 and alisertib, while VE-821 produced only a modest enhancement of alisertib-induced apoptosis. These findings indicate that the therapeutic benefit of combined mitotic kinase and DDR inhibition may depend on cell-specific molecular characteristics. Moreover, the apoptotic response to combined DDR and mitotic kinase inhibition was not uniform across all cell lines. In KKU213A cells, VE-821 did not further enhance BI2536-induced apoptosis, suggesting that the effects of DDR inhibition may depend not only on cellular context but also on the specific mitotic kinase targeted. Such variability is consistent with the molecular heterogeneity of CCA and suggests that dependence on ATM- or ATR-mediated DNA damage signaling may differ among tumor subtypes. To further investigate the underlying mechanism, we examined markers of DNA damage and apoptosis in KKU055 and HuCCA1 cells, representing the most and least responsive cell lines, respectively. Combined treatment markedly increased γH2AX accumulation and PARP cleavage relative to single-agent treatment in KKU055 cells (Figure 5A).

These molecular changes were consistent with the increase in apoptotic cell populations detected by flow cytometry, indicating that enhanced DNA damage accumulation contributes to apoptotic cell death following dual pathway inhibition. Collectively, these findings support the existence of a functional interplay between mitotic kinase signaling and the DDR machinery in CCA cells.

The enhanced efficacy of combination treatment can be explained by the complementary functions of mitotic kinases and DNA damage response signaling in maintaining genomic stability. AURKA and PLK1 coordinate centrosome maturation, spindle assembly, chromosome segregation, and checkpoint recovery during mitosis, whereas ATM and ATR orchestrate cellular responses to DNA damage and replication stress [21, 22]. Inhibition of AURKA or PLK1 is expected to induce mitotic defects, chromosomal instability, and replication-associated stress, whereas simultaneous inhibition of ATM or ATR compromises DNA repair, resulting in excessive DNA damage accumulation and activation of apoptotic pathways [23]. Consequently, combined inhibition may overwhelm DNA repair capacity, leading to the accumulation of DNA lesions and activation of apoptotic pathways. Consistent with this model, Roeschert et al. demonstrated that AURKA inhibition induces replication-associated stress and activates ATR-dependent survival signaling, whereas concurrent AURKA and ATR inhibition results in extensive DNA damage accumulation and apoptosis, supporting a synthetic lethal interaction between mitotic kinase and DDR inhibition [24]. In addition, Nam et al. reported that ATR inhibition enhances the antitumor activity of WEE1 inhibition in biliary tract cancer through increased replication stress, DNA damage accumulation, and apoptotic cell death [25]. These findings provide direct experimental evidence supporting our proposed mechanism that combined mitotic kinase and DDR inhibition can overwhelm cellular DNA repair capacity and promote apoptotic cell death. Interestingly, in HuCCA1 cells, treatment with BI2536 alone induced a robust γH2AX signal, whereas the addition of the ATR inhibitor VE-821 reduced γH2AX levels. This observation may reflect the established role of ATR as an upstream kinase involved in H2AX phosphorylation during replication stress. Previous studies have demonstrated that replication stress-induced γH2AX formation is largely ATR-dependent [26]. Therefore, inhibition of ATR may suppress H2AX phosphorylation and reduce γH2AX accumulation even when replication-associated DNA lesions persist or increase. Accordingly, a reduction in γH2AX signal following combined BI2536 and VE-821 treatment should not necessarily be interpreted as reduced DNA damage, but rather as diminished activation of ATR-dependent H2AX phosphorylation signaling.

However, in HuCCA1 cells, ATM inhibition, but not ATR inhibition, markedly enhanced γH2AX accumulation without a corresponding increase in PARP cleavage. Moreover, combination treatments did not uniformly enhance γH2AX or cleaved PARP expression relative to the corresponding single-agent treatments. These findings suggest that DNA damage accumulation alone may be insufficient to trigger robust apoptotic cell death in the HuCCA1 cell line and raise the possibility that additional pro-survival or anti-apoptotic mechanisms contribute to the relative resistance of this cell line. More broadly, the recent ENS-CCA 2026 international consensus highlighted the need for further investigation of chemoresistance mechanisms, DDR-associated vulnerabilities, and programmed cell death pathways in CCA, emphasizing the importance of understanding differential treatment responses across CCA models [5].

Several studies have demonstrated the therapeutic potential of combining AURKA inhibitors with other targeted agents. For example, MK5108, another selective AURKA inhibitor, exhibited synergistic antitumor activity when combined with the MEK inhibitor trametinib in colorectal cancer models [27]. Synergistic effects of AURKA inhibition have also been reported in combination with WEE1, CHEK1, and mTOR inhibitors in various cancer types [28-30]. Collectively, these studies support the concept that AURKA inhibition is most effective when combined with therapies that impair complementary stress-response pathways. Our findings extend this concept to cholangiocarcinoma by identifying ATM- and ATR-mediated DDR signaling as potential co-targeting partners.

Limitations should be acknowledged. First, the present study was conducted exclusively in established CCA cell lines, and therefore the therapeutic efficacy of these combinations requires validation in in vivo models. Second, the molecular determinants underlying the differential responses among CCA cell lines remain unclear and warrant further investigation. Identification of predictive biomarkers may facilitate patient stratification and improve the clinical applicability of this therapeutic strategy.

In conclusion, our findings identify mitotic kinase signaling as a potential therapeutic vulnerability in cholangiocarcinoma. Co-targeting AURKA or PLK1 together with ATM or ATR enhances DNA damage accumulation and promotes apoptotic cell death in CCA cells. Our results support further investigation of the biological and therapeutic implications of concurrent mitotic kinase and DDR pathway inhibition in CCA.

Supplementary Material

Supplementary figures and table.
https://www.jcancer.org/v17p2126s1.pdf

Acknowledgments

The present study was supported by Thailand Science Research and Innovation, Chulabhorn Research Institute Thailand (grant nos. 49890/4759792 and 53498/4821834).

Competing Interests

The authors have declared that no competing interest exists.

References

1. Sarcognato S, Sacchi D, Fassan M, Fabris L, Cadamuro M, Zanus G, et al. Cholangiocarcinoma. Pathologica. 2021; 113: 158-69.
2. Ilyas SI, Khan SA, Hallemeier CL, Kelley RK, Gores GJ. Cholangiocarcinoma - evolving concepts and therapeutic strategies. Nat Rev Clin Oncol. 2018; 15: 95-111.
3. Zanuso V, Tesini G, Valenzi E, Rimassa L. New systemic treatment options for advanced cholangiocarcinoma. J Liver Cancer. 2024; 24: 155-70.
4. Ruff SM, Pawlik TM. Clinical management of intrahepatic cholangiocarcinoma: surgical approaches and systemic therapies. Front Oncol. 2024; 14: 1321683.
5. Banales JM, Rodrigues PM, Affò S, Andersen JB, Aspichueta P, Boulter L, et al. Cholangiocarcinoma 2026: status quo, unmet needs and priorities. Nat Rev Gastroenterol Hepatol. 2026; 23: 65-96.
6. Du R, Huang C, Liu K, Li X, Dong Z. Targeting AURKA in Cancer: molecular mechanisms and opportunities for Cancer therapy. Mol Cancer. 2021; 20: 15.
7. Ma HT, Poon RYC. Aurora kinases and DNA damage response. Mutat Res. 2020; 821: 111716.
8. Zhou H, Kuang J, Zhong L, Kuo WL, Gray JW, Sahin A, et al. Tumour amplified kinase STK15/BTAK induces centrosome amplification, aneuploidy and transformation. Nat Genet. 1998; 20: 189-93.
9. Zheng D, Li J, Yan H, Zhang G, Li W, Chu E, et al. Emerging roles of Aurora-A kinase in cancer therapy resistance. Acta Pharm Sin B. 2023; 13: 2826-43.
10. Ding X, Huang T, Peng C, Ahn KS, Andersen JB, Lewinska M, et al. Therapeutic Rationale to Target Highly Expressed Aurora kinase A Conferring Poor Prognosis in Cholangiocarcinoma. J Cancer. 2020; 11: 2241-51.
11. Moolmuang B, Chaisaingmongkol J, Singhirunnusorn P, Ruchirawat M. PLK1 inhibition leads to mitotic arrest and triggers apoptosis in cholangiocarcinoma cells. Oncol Lett. 2024; 28: 316.
12. Sripa B, Leungwattanawanit S, Nitta T, Wongkham C, Bhudhisawasdi V, Puapairoj A, et al. Establishment and characterization of an opisthorchiasis-associated cholangiocarcinoma cell line (KKU-100). World J Gastroenterol. 2005; 11: 3392-7.
13. Sirisinha S, Tengchaisri T, Boonpucknavig S, Prempracha N, Ratanarapee S, Pausawasdi A. Establishment and characterization of a cholangiocarcinoma cell line from a Thai patient with intrahepatic bile duct cancer. Asian Pac J Allergy Immunol. 1991; 9: 153-7.
14. Harrington EA, Bebbington D, Moore J, Rasmussen RK, Ajose-Adeogun AO, Nakayama T, et al. VX-680, a potent and selective small-molecule inhibitor of the Aurora kinases, suppresses tumor growth in vivo. Nat Med. 2004; 10: 262-7.
15. Tyler RK, Shpiro N, Marquez R, Eyers PA. VX-680 inhibits Aurora A and Aurora B kinase activity in human cells. Cell Cycle. 2007; 6: 2846-54.
16. Cheng PT, Lin H, Cheng YC, Hsiao TH, Jhan PP, Tsai JR, et al. Alisertib inhibits acute myeloid leukemia cell growth by inhibiting STAT3 activation. Toxicol Appl Pharmacol. 2025; 502: 117449.
17. Manfredi MG, Ecsedy JA, Chakravarty A, Silverman L, Zhang M, Hoar KM, et al. Characterization of Alisertib (MLN8237), an investigational small-molecule inhibitor of aurora A kinase using novel in vivo pharmacodynamic assays. Clin Cancer Res. 2011; 17: 7614-24.
18. Zhang Y, Ma Y, Wang Y, Mukhopadhyay D, Bi Y, Ji B. Aurora kinase A inhibitor MLN8237 suppresses pancreatic cancer growth. Pancreatology. 2022; 22: 619-25.
19. Gönül Geyik Ö, Anichini G, Ulukaya E, Marra F, Raggi C. DNA Damage Response Inhibitors in Cholangiocarcinoma: Current Progress and Perspectives. Cells. 2022; 11: 1463.
20. Moolmuang B, Ruchirawat M. The antiproliferative effects of ataxia-telangiectasia mutated and ATM- and Rad3-related inhibitions and their enhancements with the cytotoxicity of DNA damaging agents in cholangiocarcinoma cells. J Pharm Pharmacol. 2021; 73: 40-51.
21. Blackford AN, Jackson SP. ATM, ATR, and DNA-PK: The Trinity at the Heart of the DNA Damage Response. Mol Cell. 2017; 66: 801-17.
22. Lens SM, Voest EE, Medema RH. Shared and separate functions of polo-like kinases and aurora kinases in cancer. Nat Rev Cancer. 2010; 10: 825-41.
23. Karnitz LM, Zou L. Molecular Pathways: Targeting ATR in Cancer Therapy. Clin Cancer Res. 2015; 21: 4780-5.
24. Roeschert I, Poon E, Henssen AG, Garcia HD, Gatti M, Giansanti C, et al. Combined inhibition of Aurora-A and ATR kinase results in regression of MYCN-amplified neuroblastoma. Nat Cancer. 2021; 2: 312-26.
25. Nam AR, Jin MH, Bang JH, Oh KS, Seo HR, Oh DY, et al. Inhibition of ATR Increases the Sensitivity to WEE1 Inhibitor in Biliary Tract Cancer. Cancer Res Treat. 2020; 52: 945-56.
26. Ward IM, Chen J. Histone H2AX is phosphorylated in an ATR-dependent manner in response to replicational stress. J Biol Chem. 2001; 276: 47759-62.
27. Sato M, Yamamoto Y, Moriwaki T, Fukuda K, Tsuchiya K. Combination of AURKA inhibitor and MEK inhibitor strongly enhances G1 arrest and induces synergistic antitumor effect on KRAS or BRAF mutant colon cancer cells. Biochem Biophys Rep. 2025; 43: 102073.
28. Alcaraz-Sanabria A, Nieto-Jiménez C, Corrales-Sánchez V, Serrano-Oviedo L, Andrés-Pretel F, Montero JC, et al. Synthetic Lethality Interaction Between Aurora Kinases and CHEK1 Inhibitors in Ovarian Cancer. Mol Cancer Ther. 2017; 16: 2552-62.
29. Brewer SKJ, Demicco EG, Lusby K, Ghadimi MP, Belousov R, Young E, et al. Dual targeting of mTOR and aurora-A kinase for the treatment of uterine Leiomyosarcoma. Clin Cancer Res. 2012; 18: 4633-45.
30. Lee JW, Parameswaran J, Sandoval-Schaefer T, Eoh KJ, Yang DH, Zhu F, et al. Combined Aurora Kinase A (AURKA) and WEE1 Inhibition Demonstrates Synergistic Antitumor Effect in Squamous Cell Carcinoma of the Head and Neck. Clin Cancer Res. 2019; 25: 3430-42.